Relationship of Optical and Acoustic Emissions to Laser Weld Penetration

Optical and acoustic emissions are shown to be related to laser weld quality and also to each other

BY DAVE FARSON, AFSAR ALI AND YAN SANG

ABSTRACT. Detection and analysis of optical, acoustic and plasma charge emissions from laser beam welds is a promising approach for quality monitoring. In this work, the airborne acoustic and optical-wavelength electromagnetic ("light") emissions from laser welds were studied. A matrix of travel speed and CO_2 laser power settings was used to generate bead-on-plate welds in cold-rolled low-carbon steel sheet metal. The power/travel matrix-generated welds having partial penetration, "moderate" full penetration (visually sound welds) and "excessive" penetration (relatively wide weld beads with undercut due to drop-through of the molten pool). The intensity of the light emitted from the weld area was found to vary with process parameters, exhibiting a local minimum for moderately full-penetration welds. The RMS amplitude of the acoustic energy was found to have a local maximum for these same moderate full-penetration conditions. The relationship between the optical and acoustic signals was investigated and it was found that the acoustic signal was approximately proportional to the time derivative of the optical signal. The front-side light emission signal was also found to vary inversely with back-side light emission.

Introduction

The use of the laser as a tool for welding, and other industrial material processing, continues to grow steadily. However, commercial users have long desired a means of in-process monitoring to ensure laser weld quality. Direct measurement of weld quality characteristics (such as width, penetration depth or shape) in real-time is difficult in many cases. An alternative approach is to measure process emissions, including acoustic and electromagnetic waves and charged particle flux. Although there has been considerable research into emission-based monitors (some of which is discussed in the next section), there are still questions as to the correlation between emissions and weld characteristics. One drawback of this monitoring approach is that the emission signals are only indirectly related to weld quality.

The work described in this paper shows that the optical energy ("light") emitted during laser beam welding, for example, depends not only on the degree of weld penetration (whether the weld is full or partial penetration) but also on laser power, travel speed, material and other characteristics. Consequently, implementation of emission-based monitors currently requires that the user execute a large number of test welds representative of the specific application of interest to gain information about the relationship between emissions and weld quality characteristics. A more predictive understanding of relationships between laser weld emissions and quality characteristics of interest (e.g., penetration) will allow quicker, less expensive implementation of emission-based monitors with better reliability.

The research described in this paper focused on several relationships of interest to those attempting to design emission-based laser weld quality monitors. The relationship between weld quality and optical and acoustic emissions, two types commonly employed for weld quality monitoring, was experimentally investigated. One objective was to analyze optical and acoustic emission data to determine if correspondence between signal characteristics such as emission amplitude (measured by signal amplitude) and fluctuation (measured by signal standard deviation) and weld penetration could be established in spite of variations in process parameters (e.g., power and travel speed). As will be noted below, it is known that emission characteristics such as these can be correlated to weld penetration within certain ranges of process parameters. This work investigated relatively broad ranges of power and travel speed to assess the "globalness" of any observed emission/penetration correlations. Another objective was to determine whether or not the front-side optical signals contained unique features corresponding to full penetration "events." Such features would be potentially useful for monitoring weld penetration since they would (presumably) be absent in partial penetration weld signals. A final goal was to ascertain whether or not the optical and acoustic emissions were correlated to each other. A fundamental question is the degree to which the two emissions provide redundant or independent information about weld penetration. This information is useful in the design and application of monitoring systems that simultaneously analyze both the acoustic and optical emissions.

KEY WORDS

Laser Beam Welding
Emission-Based Monitors
Optical Emissions
Acoustic Emissions
Full-Penetration Welds
Partial-Penetration Welds

DAVE FARSON, AFSAR ALI and YAN SANG are with The Ohio State University, Dept. of Industrial, Welding and Systems Engineering, Columbus, Ohio.

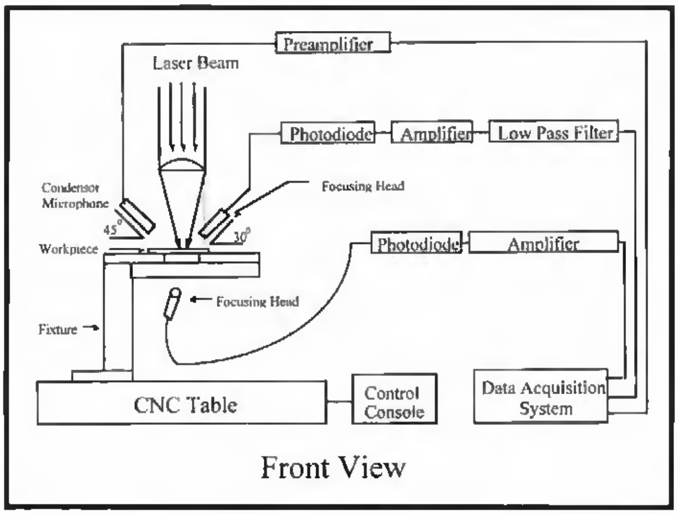

Fig. 1 — Experimental apparatus including the data acquisition system.

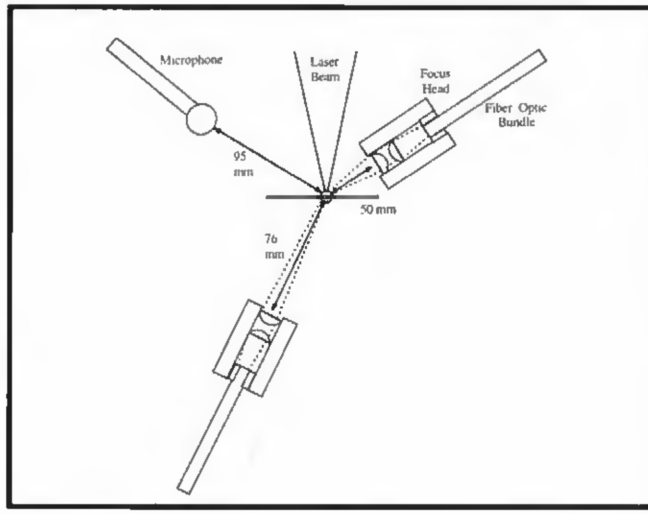

Fig. 2 — Sensor position.

Background

In emission-based monitoring, laser welding process information is obtained by measuring and characterizing the various forms of energy that propagate from the laser-material interaction site, *i.e.*, the "keyhole." There are a variety of such emissions. Electromagnetic radiation from ultraviolet (UV) to infrared (IR) wavelengths is generated by the partially ionized plume and molten material. Airborne acoustic waves are generated by the unsteady displacement of the surrounding air due to evaporation, heating and expansion of material. Acoustic waves are also generated in the weld base metal by thermal strains and/or microstructural changes, evaporation recoil pressure and, perhaps, other effects. Transport of charged particles (*i.e.*, electrons and ions) can also produce measurable current flows and/or charge buildup in the target material or objects present near the plume. Since all of these emissions depend upon physical phenomena occurring at the laser-material interaction site, their characteristics (*e.g.*, time-varying amplitude, spatial distribution, etc.) may be indirectly related to final process quality measures that are also dependent upon physical phenomena at the interaction site. This investigation was concerned mainly with airborne acoustic and optical emissions. A more detailed discussion of past results relevant to these two topics follows.

Monitoring of Weld Quality with Airborne Acoustic Emissions

In a very early work, Jon (Ref. 1) described one of the first investigations in the field of laser weld acoustic monitoring. Airborne acoustic energy was measured with a piezoelectric transducer attached to a flat plate suspended just above the laser-material interaction site. As is common in analyzing acoustic emission in solids, "counts" were used as a measure of signal intensity. It was found that a relatively low number of counts was associated with several weld defect conditions, including shallow (<20% penetration due to out-of-focus condition), drilling, wide root opening and misaligned welds. Similarly, Orlicke, *et al.* (Ref. 2), demonstrated detection of out-of-focus and wide fit-up root opening conditions using thresholding of the total detected airborne acoustic energy signal.

Li and Steen (Ref. 3) studied the root mean square (RMS) amplitude of airborne acoustic signals from bead-on-plate welds as a function of laser power and travel speed. The acoustic emissions were detected using a transducer mounted on a concentric gas nozzle. Starting with relatively high heat input conditions (high power/low travel speed), the acoustic intensity gradually increased to the maximum with increased power or decreased travel speed. The acoustic intensity then decreased as power was further increased or travel speed was further decreased.

The time-based frequency spectrum of acoustic emissions contains more information than either "event" analysis or simple amplitude measurements. In a recent work, Duley and Mao (Ref. 4) investigated the effect of surface condition on the airborne acoustic spectra observed during CO_2 laser welding of 1100 aluminum alloy. Acoustic power at frequencies under 10 kHz generally increased with increased incident laser power. Based on experimental results and a theoretical analysis of the dynamics of the liquid-filled weld keyhole, resonance spikes that appeared in the spectral band from 3–9 kHz were attributed to motion of molten aluminum within the keyhole.

Farson, Fang and Kern (Ref. 5) developed a rudimentary laser weld penetration control based on airborne acoustic signal measurements. Acoustic emissions were detected with a microphone and the microphone output voltage was digitized. The Fourier transform of the sampled signal was input to a neural network. Using spectra collected from a matrix of experimental conditions, the network was trained to discriminate between full- and partial-penetration welds. The neural network classifications were then input to a fuzzy logic controller that generated process speed offsets needed to maintain full penetration.

Monitoring Laser Weld Quality with Optical Emissions

Ishide, *et al.* (Ref. 6), describe the development and experimental characterization of an optical sensing system for monitoring of a fiber-delivered Nd:YAG welding process. The design of the monitoring system is innovative. The power fiber was surrounded with a circular array of smaller monitoring fibers. The light transmitted by the sensing fibers was filtered to a narrow pass-band centered at 940 nm and detected with a silicon photodiode. He observed that the average value of the diode signal increased approximately linearly with incident laser power. Thus, delivered power drops caused by damaged beam delivery optics were observed to cause a noticeable drop in sensor signal.

Beyer, *et al.* (Ref. 7), reported laser

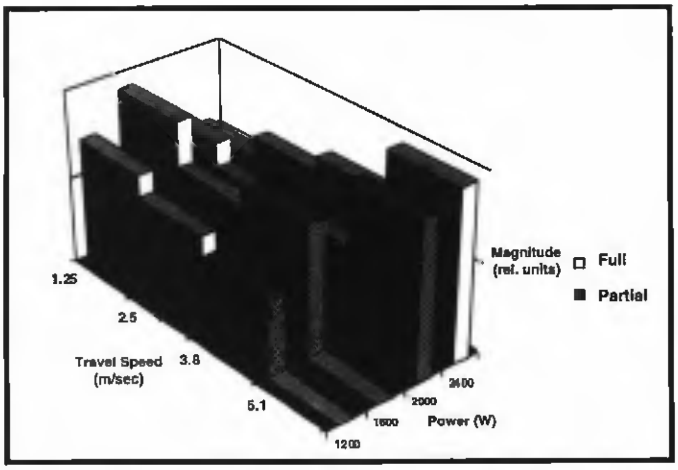

Fig. 3 — RMS amplitude of the optical signal as a function of travel speed and power for full- and partial-penetration welds.

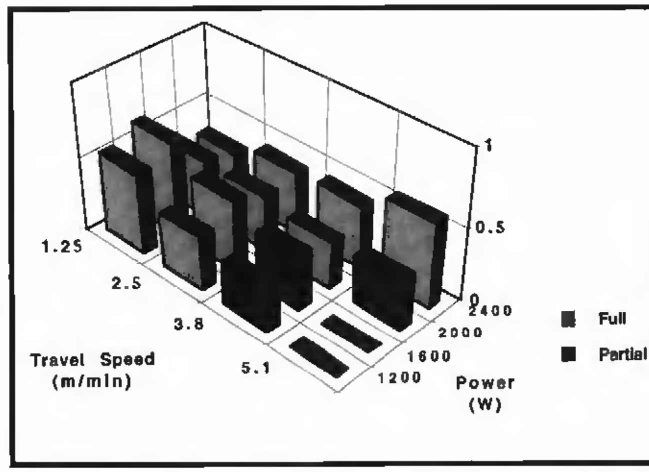

Fig. 4 — Standard deviation of the optical signal as a function of travel speed and power for full- and partial-penetration welds.

weld monitoring results obtained using a related approach. In this work, the development of an optical monitoring system for detecting lack of penetration and gapping in sheet metal lap joint welds is described. The system used a backpropagation neural network to detect defect conditions, such as partial penetration and lap weld gapping by classifying the amplitude of the spectrum of the signals. Fairly good monitoring results (approximately 98% reliable) were obtained.

Another optical monitoring system was described by Kluft, *et al.* (Ref. 8). A photodiode detector filtered to blue wavelengths (450–550 nm) was used to measure optical emissions. The time-based frequency amplitude spectrum of the photodiode signal was analyzed for various welding conditions. It was observed that the ratio of high frequency (500 Hz to 10 kHz) to low frequency (0 to 500 Hz) energy in the spectrum changed with penetration. The ratio was larger when welding at full penetration than it was for partial penetration. This relationship was found to hold for variations in penetration caused by workpiece thickness changes and also by focal point elevation changes.

Leong, *et al.* (Ref. 9), describes correlations between infrared optical emission intensity and weld characteristics. A linear relationship was found to exist between optical signal DC amplitude and weld penetration depth. In these tests, the weld penetration depth (all welds were partial penetration) was varied by changing the CO_2 laser CW power. Changes in gas shielding configuration and the presence of oil on the base metal surface were found to cause significant changes in the AC amplitude of the infrared optical emission. Spatter was also found to influence the AC amplitude of the emission.

Finally, Shibata (Ref. 10) briefly describes a system for monitoring laser sheet metal welding based on optical emissions. The system used two photodiode detectors to measure optical emissions emanating at different angles from the base metal surface, one nearly perpendicular and the other nearly parallel. Correlations between optical emission signals and weld quality were obtained from "large volumes" of experimental data obtained during production welding. It was indicated that the plasma monitor was useful for detecting weld pits, bead humping, joint mismatch and lack of penetration.

Acoustic and Optical Emission Relationships

It is natural and potentially useful to inquire about the relationship between airborne acoustic and optical emissions, the two emissions most commonly used for weld monitoring. Experimental work regarding such relationships was done by Gatzweiler, Maischner, Derichs and Beyer (Ref. 11). They made full- and partial-penetration welds on steel base material using a CO_2 laser. Visual inspection of experimental data showed that photodiode signals representing plume emissions were temporally related to the signals from an instrument microphone. However, this relationship was not investigated further in their work.

In another early work, Lewis and Dixon (Ref. 12) report on monitoring of laser welds with a microphone and optical photomultiplier sensor. The welds were made on aluminum, gold and stainless steel using single pulses from a 400-W average power Nd:YAG laser. Strong variations in sound pressure and noticeable variations in plasma optical emission were noted. Although no note was made of the fact, a cursory comparison of sensor data reveals some correspondence between the optical and acoustical signals.

Experimental Procedure

A Fanuc 3-kW CW CO_2 laser was used to produce bead-on-plate welds on carbon steel sheet material. The experimental setup is shown in Fig. 1. The fixture (including the workpiece) was mounted on a CNC x-y table to provide mobility. The laser beam was focused on the surface of the workpiece at a 90-deg angle of incidence. The laser beam had a spot size of about 0.2 mm, which resulted in power density on the order of 106 W/cm^2.

Three separate sensors were used to monitor process emissions during welding. A silicon photodiode with optical bandwidth of 0.3~1 μm and time bandwidth of 0~200 kHz was used for monitoring front-side optical emissions. An identical photodiode was used to monitor backside optical emissions. A condenser microphone with a bandwidth of 20 Hz to 20 kHz was used to monitor airborne acoustic emissions (*i.e.*, sound pressure waves).

The arrangement of the sensors is shown in Fig. 2. Light emitted from the front and back sides of the weld area was collected and injected into fused silica fiber bundles with two-lens focus assemblies and transmitted via the fiber bundles to the photodiode detectors. The two-lens focusing system had a magnification of 1.28 and the diameter of the

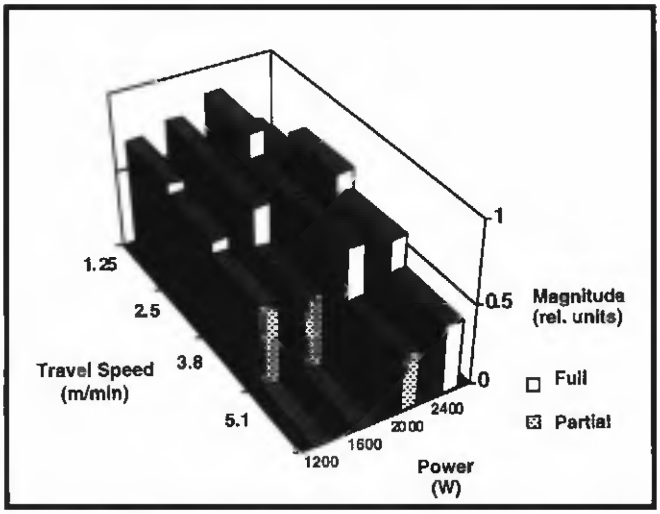

Fig. 5 — RMS amplitude of the acoustic signal as a function of travel speed and power for full- and partial-penetration welds.

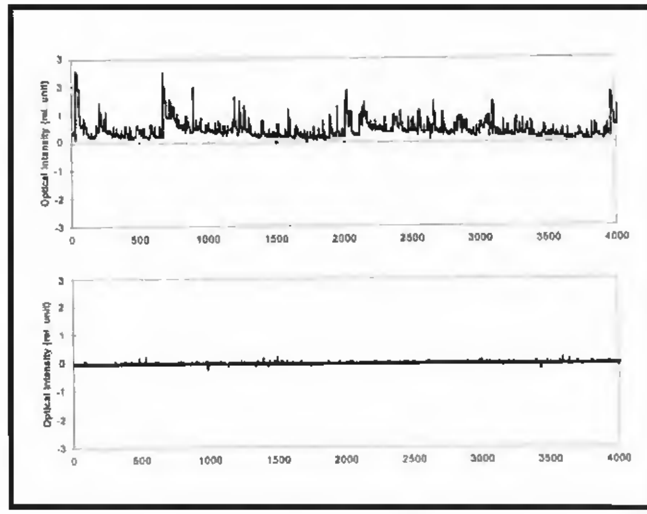

Fig. 6 — Backside light intensity for full (top) and partial (bottom) penetration welds.

fiber-optic bundle was 1.6 mm. Therefore, the system collected light from an area with a diameter of 2.0 mm (at the focal plane) and within a solid angle of approximately 0.15 steradian. The collection area was centered approximately on the keyhole opening.

A personal computer with an analog-to-digital converter card, configured as shown in Fig. 1, was used to acquire sensor output voltage. Each of the three sensor signals was sampled at a rate of 50 kHz for a total time period of 0.32 s (resulting in a sample set size of 16,000 points for each of the three sensors). To prevent aliasing, the front-side light signal was filtered with an eighth-order low pass filter with cut-off frequency of 20 kHz before it was input to the data acquisition system. The high-frequency band limit of the microphone (equal to 20 kHz) prevented aliasing of the acoustic signal without the need for additional filtering.

A full matrix of power and travel speed settings was used to generate both full- and partial-penetration welds. Power settings were 1200, 1600 and 2400 W. Travel speeds were 1.25, 2.5, 3.8 and 5.1 m/min. Helium shielding gas was delivered both coaxially and from a side shield at a combined flow rate of 20 ft^3/h. At some low power/high travel speed combinations, the energy density was insufficient for coupling, and conduction mode (rather than keyhole mode) welds resulted. The material used for the experiments was 1.4-mm-thick cold-rolled low-carbon steel sheet. The welding parameters are summarized in Table 1.

Results and Discussion

The optical and acoustic signal sample sets were first analyzed by simple statistical measures to determine if correlations between signal characteristics and full/partial penetration conditions could be identified. The RMS value, given as

$$s_{RMS} = \sqrt{\frac{\sum_{i=1}^{n} s_i^2}{n}}$$

where s_{rms} = signal root-mean-square value (acoustic or light), n = total number of samples in set (*i.e.*, 16,000) and s_i = sample value, was taken as a measure of the amplitude of the signals. Using these RMS values, three-dimensional response plots for both acoustic and light signals were constructed.

The response plots for variations of the RMS value of the optical signal with laser travel speed and power are shown in Fig. 3. It appears that a local minimum in optical signal RMS amplitude is obtained at what might be described as "moderate" full-penetration conditions (*i.e.*, at conditions where the weld is fully penetrating but of sufficiently small width that the top surface is not significantly undercut by weld pool drop through). The data series obtained by varying travel speed at a constant power of 1600 or 2000 W both show this minimum in the light emission at moderate full-penetration conditions. When travel speed is increased or decreased from this point, the light emission increases noticeably. When the travel speed was 5.1 m/min and power was 1200 or 1600 W, no keyhole was formed and the optical emissions were very low. Also, generally lower emission levels were ob-

Table 1 — Welding Parameters

Weld Number	Laser Power (W)	Travel Speed (m/min)	Penetration (Visual Inspection)
1	2400	1.25	Full
2	2400	2.5	Full
3	2400	3.8	Full
4	2400	5.1	Full
5	2000	1.25	Full
6	2000	2.5	Full
7	2000	3.8	Full
8	2000	5.1	Partial
9	1600	1.25	Full
10	1600	2.5	Full
11	1600	3.8	Partial
12	1600	5.1	No coupling
13	1200	1.25	Full
14	1200	2.5	Full
15	1200	3.8	Partial
16	1200	5.1	No coupling

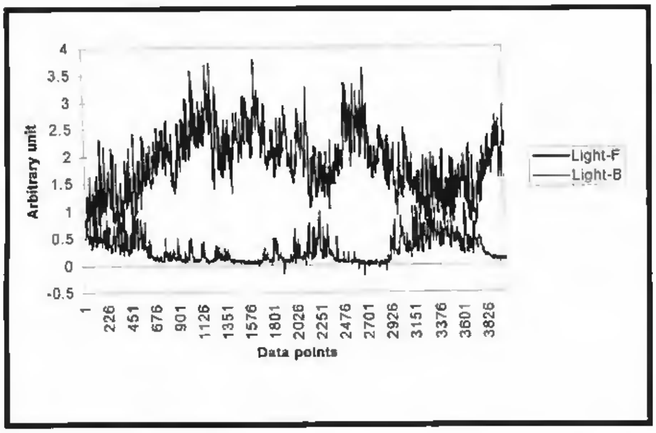

Fig. 7 — Front-side and backside light signal relationship for a full-penetration weld.

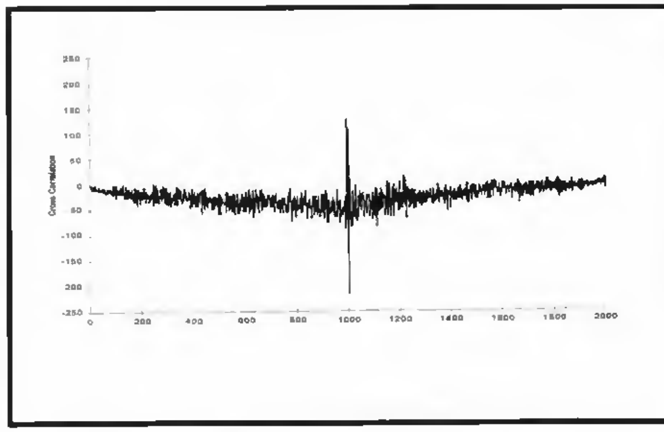

Fig. 8 — Cross correlation between light and sound signals.

served when travel speed was at the lower range of levels in the test matrix and power was at or near its highest values. This is most clearly observed in the data series for varying travel speeds at a power of 2400 W, where the optical signal amplitude steadily dropped as travel speed was decreased.

The results shown in Fig. 3 have important implications for the design and application of laser penetration monitoring systems. Undoubtedly the simplest strategy for discriminating between full- and partial-penetration welds based on their optical emission is to compare the optical emission amplitude to a fixed threshold level. The above results indicate that such a strategy will be successful only for laser power and travel speed combinations within certain ranges. For example, the results show that full- and partial-penetration welds made at powers of 1600 and 2000 W and travel speeds of 2.5 and 3.8 m/min could be successfully discriminated using a fixed threshold since, in this parameter range, partial-penetration welds had consistently higher optical emission amplitudes than full-penetration welds. However, outside of this power/travel speed range, examples of welds having optical emission amplitudes that would be misclassified by such a simple threshold are evident. In fact, it is interesting to note that the partial-penetration weld made at a power of 1200 W and a travel speed of 3.8 m/min had lower optical emission amplitude than the full-penetration weld made at a power of 1200 W and travel speed of 2.5 m/min, the opposite of the trend noted above. These results imply that laser weld monitoring systems that determine degree of penetration by comparing the optical signal amplitude to a threshold will generally require adjustment of both the threshold level and comparison rules to be applicable over a wide range of process conditions.

The marked increase in optical emission noted when comparing keyhole welds to conduction-mode welds appeared (from visual observation) to be related to an increase in plume size. The increased plume size may stem from increased absorption of laser energy in the material due to keyhole effects, leading to greater evaporation of iron into the plume. Since iron has a relatively low ionization potential, its enrichment in the plume should lead to more excited and ionized species and, hence, more radiation by de-excitation and deionization events. Also, the increased charged species concentration leads to increased absorption of laser energy in the plume, which promotes further ionization, so the increased optical emission due to iron enrichment should be self-perpetuating to some degree. Reasons for the nonmonotonic variation of optical emission with changes in power, travel speed and degree of penetration require further investigation before conclusive explanations can be given.

Another emission signal characteristic that has been proposed for weld quality monitoring purposes is standard deviation. The standard deviation of the optical signal for the various conditions in the power/travel speed test matrix is plotted in Fig. 4. This data shows the maximum variation in the optical signal tended to be associated with full-penetration welding conditions. However, the difference in RMS amplitude between full- and partial-penetration welds was small in some cases (e.g., the data series with travel speed equal to 3.8 m/min). This result implies a weld penetration discrimination approach based on comparison of the optical signal standard deviation to a fixed threshold could be successful in certain ranges of power and travel speed. For example, the data taken at 1200 and 1600 W and 2.5 and 3.8 m/min clearly show standard deviation was higher for full-penetration welds than partial-penetration welds. However, the "rule" fails for welds outside of this parameter range. For example, the weld made at 1600 W and 3.8 m/min has a relatively low standard deviation that would be misclassified by a threshold suitable for the previous power/travel speed range. Thus, thresholding the standard deviation of the optical signal may yield desired results in selected parameter ranges but will generally not be accurate if applied across a wider parameter range.

The acoustic RMS amplitude response plot for welds made at various combinations of power and travel speed is displayed in Fig. 5. The trend evident in this data is somewhat similar to that observed for the standard deviation of the optical emission: the airborne acoustic signal attained its maximum RMS level during full-penetration welding. The acoustic amplitude data series obtained by varying travel speed at a power level of 2400 W reveals a maximum in the RMS acoustic emission at 2.5 m/min, with lower emission at both faster and slower travel speeds. This behavior was also observed for the data series obtained by varying power at a constant travel speed of 1.25 m/min. It is important to note that a single threshold value that will discriminate full- and partial-penetration welds based on acoustic signal magnitude is not possible in general. However, just as in the case of the optical signal, such a strategy is viable in certain regions of the power/travel speed parameter space. In particular, the transition from full to partial penetration at the high travel speed of 5.1 m/s (due to a power increase from 2000 to 2400 W) was correlated with an especially pronounced increase in acoustic signal magnitude.

Two plots of the time-variation the

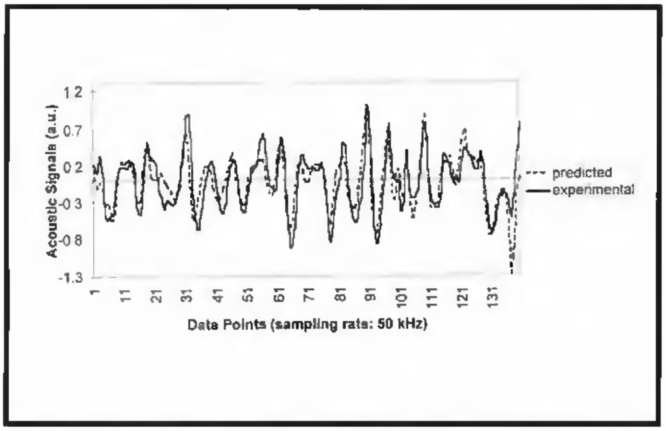

Fig. 9 — Comparison of the derivative of the light to the acoustic signal for a partial-penetration weld (r = 3.16).

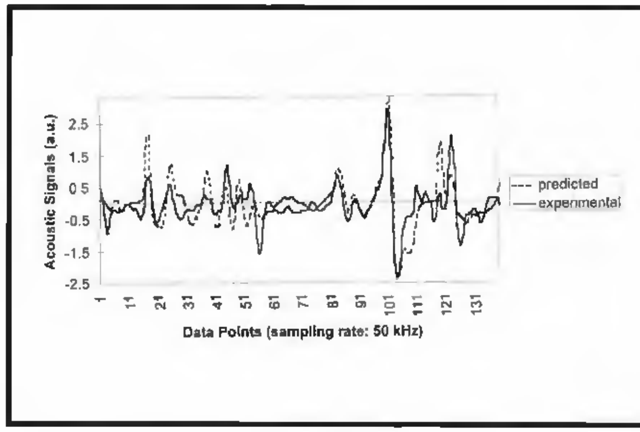

Fig. 10 — Comparison of the derivative of the light signal to the acoustic signal for a full-penetration weld (r = 1.38).

backside optical signal magnitude are shown in Fig. 6. Partial-penetration welds generated no significant backside optical emissions. On the other hand, full-penetration welds were generally characterized by large magnitude, highly fluctuating backside optical emissions. This relationship between backside light emission and weld penetration is well known and backside optical sensors have sometimes been used for weld penetration monitoring because of this correspondence. However, in most cases it is not practical to collect the backside optical signal because of restricted access or other reasons.

The primary reason for studying the backside optical emission in this work was to determine whether or not any front-side signal features that uniquely correspond to full-penetration welding could be identified. Since the backside light signal provides some indication of the status of the keyhole, a detailed examination of the time variation of both front-side and backside optical signals could possibly reveal time-domain front-side signal fluctuations that correspond to periods of high- or low-backside emission. A representative plot of front-side and backside light signals is shown in Fig. 7.

The results shown in Fig. 7 indicate that, on average, front-side and backside light signals tend to vary inversely. There is a clear trend for the average front-side signal magnitude to be high at times when the backside signal average amplitude is low and vice-versa. However, the standard deviation of both signals is quite high, so the relationship is better in the average rather than on a sample-by-sample basis. Visual inspection and cross-correlation analysis failed to identify any particular time-domain features in the front-side optical signal that reliably indicated the presence or absence of full penetration or that were consistently related to peaks in the backside optical emission signal.

Relation between Light and Acoustic Signals

One thrust of ongoing work in emission-based monitoring is the development of multiple-sensor systems. In designing such systems, it is helpful to understand the similarities and differences in the signals produced by various emission sensors. The light/sound signals were analyzed to determine if there was a deterministic connection between the two. As a first step, a correlation integral (Ref. 13) was performed on the time samples as a rough indicator for the presence of a relationship. The magnitude of the correlation integral of two fluctuating signals is high when the signals fluctuate in unison and is low if there is little relationship between the two. Additionally, the correlation is negative if the signals fluctuate out of phase (in opposition) to each other but is positive if the fluctuations are in phase. The cross-correlation integral of simultaneous light and sound samples from the same weld is shown in Fig. 8. The relatively high magnitudes (both positive and negative) indicate that the two signals were highly related when the sound signal was shifted in time by an amount corresponding to the propagation time from the weld keyhole to the microphone. The positive and negative peaks occurred next to each other, separated by a phase shift corresponding to one time period of the dominant frequency of oscillation of the two signals.

Next, autoregressive moving average (ARMA) modeling (Ref. 13) of the time-shifted front-side light and sound signals was used to quantify the light/sound relationship. This analysis showed that the following equation adequately modeled the relationship between the acoustic signal a(t) and the optical signal o(t):

$$a(t) \approx 2.5 \frac{d}{dt} o(t)$$

Very simply, the acoustic signal was found to be proportional to the time derivative of the optical signal. The relationship is illustrated for some representative cases in Figs. 9 and 10.

The match between the experimental and predicted acoustic signals is very striking in Fig. 9, but somewhat less so in Fig. 10. These figures were selected to represent the best and the worst of the

Table 2—Signal-to-Noise Ratio (r) for Various Welding Conditions

Laser Power (W)	Travel Speed (m/min)	Penetration	Signal-to-Noise Ratio (r)
1200	1.25	Full	3.11
1200	1.25	Full	1.39
1200	2.5	Partial	3.16
2000	3.8	Full	2.68
2000	5.1	Partial	3.13
1600	1.25	Full	2.03
1600	2.5	Full	2.41
1600	2.5	Full	1.38
1600	3.8	Partial	2.24

correlations that were observed. The match between the two signals can be examined more quantitatively using a signal-to-noise ratio (r), expressed as

$$r = \frac{\sum_{i}^{n} y_i^2}{\sum_{i}^{n} \varepsilon_i^2}$$

where y_i is the experimental acoustic signal, $\varepsilon_i = y_i - \hat{y}_i$ is the error between experimental and predicted signals and $\hat{y}_i$ is the predicted acoustic signal. Values of signal to noise ratio for a variety of conditions are listed in Table 2.

This result could have important implications for design of multiple-sensor quality monitoring systems. Under the experimental conditions that were used in these experiments, the optical signal alone is shown to contain a large amount of the information that is supplied by the acoustic signal. However, whether or not the acoustic sensor can be replaced by the optical signal has not been firmly established as there are still significant discrepancies between the actual acoustic signal and that derived from the optical signal.

Conclusions

The experimental results indicate that the amplitude of the optical-wavelength electromagnetic emissions vary with travel speed and power. Near some power and travel speed combinations (those in the middle of the parameter ranges that were tested) a transition from full to partial penetration was accompanied by a significant increase in emitted light. However, near the edges of the parameter matrix, the opposite behavior could be observed (*i.e.*, the magnitude of the optical signal decreased during the full-to-partial-penetration transition). These observations highlight the point that simple fixed rules and signal magnitude thresholds are not generally applicable for laser weld penetration detection. The airborne acoustic signal was found to be loudest at moderate full-penetration conditions and was observed to decrease when weld penetration transitioned from full to partial. Again, the size of the decrease was dependent upon the travel speed/power values. Finally, it was observed that the time derivative of the optical signal was highly correlated to the acoustic signal.

References

1. Jon, M. C. 1985. Noncontact acoustic emission monitoring of laser beam welding. *Welding Journal* 64(9): 43-s to 48-s.

2. Orlicke, H., Morgenstern, H., and Meyendorf, N. 1991. Process monitoring in welding with solid state lasers by sound emission analysis. *Welding and Cutting*, vol. 12, pp. E269–E272.

3. Li, L., and Steen, W. 1992. Noncontact acoustic emission monitoring during laser processing. *Proc. ICALEO*. Laser Institute of America, pp. 719–725.

4. Duley, W. W., and Mao, Y. L. 1994. Effect of surface condition on acoustic emission during welding of aluminium with CO_2 laser radiation. *Jour. Phys. D-Appl. Phys.* 27(7): 1379–1383.

5. Farson, D., Fang, K., and Kern, J. 1991. Intelligent laser welding control, *Proc. ICALEO*. Laser Insitute of America, pp. 105–117.

6. Ishide, T., Nagura, Y., Matsumoto, O., Sakamoto, N., Nagashima, T., and Ylkoyama, A. 1994. Compact YAG laser welding system and its in-process monitoring in sleeving technology. *Maintenance and Repair Welding in Power Plants V*, EPRI and AWS. pp. 97–103.

7. Beyer, E., Maischner, D., and Kratzsch, Ch. 1994. A neural network to analyze plasma fluctuations with the aim to determine the degree of full penetration in laser welding. *Proc. ICALEO*. Laser Institute of America, pp. 51–57.

8. Kluft, W., Boerger, P., and Schwartz, R. 1996. *On-line monitoring of laser welding of sheet metal by special evaluation of plasma radiation*. *Proc. ICALEO — Lasers and Electro-Optics for Automotive Manufacturing*. Laser Institute of America, pp. 62–71.

9. Leong, K. 1997. Low cost laser weld monitoring system. *Proc. Automotive Laser Applications Workshop*. Univ. Michigan Press, pp. 26–35.

10. Shibata, K. 1996. Tailored blank welding at Nissan. *Proc. ECLAT '96*, DGM Informationsgesellschaft, pp. 49–58.

11. Gatzweiler, W., Maischner, F., Derichs, C., and Beyer, E. 1989. Model of dynamic behaviour in laser beam welding. *Proc. SPIE*, vol. 1132, pp. 157–165.

12. Lewis, G. K., and Dixon, R. D. 1985. Plasma monitoring of laser beam welds. *Welding Journal* 64(2): 49-s to 54-s.

13. Farson, D., Sang, Y., and Ali, A. 1997. Relationship between airborne acoustic and optical emissions during laser welding. *Jour. Laser App.* 9 (2): 87–94.